

Disentangled Interpretable Representation for Efficient Long-term Time Series Forecasting

Yuang Zhao*, Tianyu Li*, Jiadong Chen[†], Shenrong Ye*, Fuxin Jiang[‡], Tieying Zhang[‡], Xiaofeng Gao^{†§}

* *SJTU Paris Elite Institute of Technology, Shanghai Jiao Tong University*

[†] *Department of Computer Science and Engineering, Shanghai Jiao Tong University*

[‡] *ByteDance Inc.*

{zhaoyuang, hugo_li, , olivier.9928}@sjtu.edu.cn, gao-xf@cs.sjtu.edu.cn

{jiangfuxin, tieying.zhang}@bytedance.com

Abstract—Industry 5.0 introduces new challenges for Long-term Time Series Forecasting (LTSF), characterized by high-dimensional, high-resolution data and high-stakes application scenarios. Against this backdrop, developing efficient and interpretable models for LTSF becomes a key challenge. Existing deep learning and linear models often suffer from excessive parameter complexity and lack intuitive interpretability. To address these issues, we propose DiPE-Linear, a Disentangled interpretable Parameter-Efficient Linear network. DiPE-Linear incorporates three temporal components: Static Frequential Attention (SFA), Static Temporal Attention (STA), and Independent Frequential Mapping (IFM). These components alternate between learning in the frequency and time domains to achieve disentangled interpretability. The decomposed model structure reduces parameter complexity from quadratic in fully connected networks (FCs) to linear and computational complexity from quadratic to log-linear. Additionally, a Low-Rank Weight Sharing policy enhances the model’s ability to handle multivariate series. Despite operating within a subspace of FCs with limited expressive capacity, DiPE-Linear demonstrates comparable or superior performance to both FCs and nonlinear models across multiple open-source and real-world LTSF datasets, validating the effectiveness of its sophisticatedly designed structure. The combination of efficiency, accuracy, and interpretability makes DiPE-Linear a strong candidate for advancing LTSF in both research and real-world applications. The source code is available at <https://github.com/wintertee/DiPE-Linear>.

Index Terms—Time series analysis, Time series forecasting, Efficient neural network, Interpretable artificial intelligence

I. INTRODUCTION

Long-term Time Series Forecasting (LTSF) is of significant importance in numerous domains, particularly in industrial applications such as cloud computing [1], [2], energy optimization [3], [4], and manufacturing [5], [6]. Recent advancements in deep learning, including Recurrent Neural Networks (RNNs) [7], Convolutional Neural Networks (CNNs) [8]–[11], Transformers [12]–[20], Multilayer Perceptrons (MLPs) [21]–[26] and Fully Connected linear models (FCs) [27]–[29] have demonstrated promising performance for LTSF tasks. With the advent of Industry 5.0 and the era of big data, time-series data processing faces three primary challenges:

Preprint. Under review.

This work has been submitted to the IEEE for possible publication. Copyright may be transferred without notice, after which this version may no longer be accessible.

[§]Corresponding author.

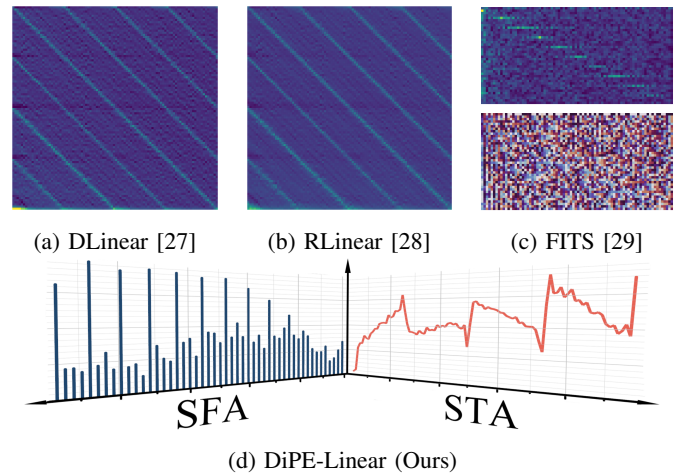


Fig. 1: Weight visualization on the ETTh1 dataset under input length $L = 96$ and horizon $L' = 96$ setting. Figs. 1a and 1b display time-domain weights. Fig. 1c shows amplitude and phase in the frequency domain. Fig. 1d shows disentangled representation of DiPE-Linear in both frequency domain (left, Static Frequential Attention, SFA) and time domain (right, Static Temporal Attention, STA).

high dimensionality, high resolution, and regulatory industrial scenarios. As regulatory emphasis on carbon footprint and trustworthiness increases [30], developing an efficient and interpretable time-series forecasting method has emerged as a critical challenge.

Long-term forecasting for high-resolution time-series data remains challenging. Metrics like CPU load and network traffic in cloud environments are sampled at minute intervals, yet predictions must span days to support proactive resource allocation [20], [31], [32]. Similarly, advanced sensors in industrial settings generate vast minute-level data, requiring accurate long-term forecasting for equipment monitoring and operational optimization [33]. Existing methods face key limitations: RNNs struggle with parallelization [7], CNNs (e.g., TimesNet [11]) impose high computational costs, and Transformers, despite linear complexity improvements [16], [17], often overfit on long input sequences [27]. Fully connected

models offer simplicity and competitive performance but suffer from quadratic complexity and parameter redundancy (Figs. 1a to 1c). This raises the pivotal question: **How can a model achieve parameter efficiency to effectively handle the challenges of long-term forecasting for high-resolution data?**

In high-stakes industrial scenarios, interpretability are indispensable requirements for achieving trustworthy AI [34], [35]. In this context, domain experts must understand the model to trust its predictions. While leading deep learning models offer impressive precision, their black-box nature significantly undermines user trust. Fully connected linear models, by contrast, provide better interpretability by design. However, it remains challenging to fully and directly understand the features encoded by these models through their two-dimensional weight matrices, whether represented in the time domain (Figs. 1a and 1b) or frequency domain (Fig. 1c). This introduces the second key question: **How can a model ensure interpretability, enabling domain experts to understand and trust its predictions in high-stakes industrial applications?**

To address these challenges, we revisit the performance of FCs in LTSF, seeking inductive biases to reduce complexity and enhance interpretability. Figs. 1a and 1b reveals that highly correlated weights along the diagonal suggest parameter redundancy in the time domain, while the high noise in off-diagonal regions in the frequency domain as shown in Fig. 1c indicates the independence of frequency components. This motivates our frequency independence hypothesis. Furthermore, time series often exhibit varying contributions of input time points to future predictions; for example, the most recent data typically plays a greater role in predicting future values. Thus, modeling the temporal significance of input sequences is crucial. Similarly, different frequency components contribute unequally [36], with significant frequencies often possessing higher signal-to-noise ratios and deserving more model attention. Finally, in multivariate time series, variable dependencies must be captured in an explainable manner, as variables may either share patterns or act independently.

Based on the aforementioned motivations, we propose a novel **Disentangled interpretable and Parameter-Efficient Linear model (DiPE-Linear)** for long-term time series forecasting. As a deep linear model, it is structured into three interpretable linear sub-modules: **Static Frequential Attention (SFA)**, **Static Temporal Attention (STA)**, and **Independent Frequential Mapping (IFM)**. The SFA module extracts and enhances prominent frequencies in the frequency domain, and the STA module selects input time points in the time domain that are strongly correlated with the predicted sequence. Meanwhile, the IFM module assumes independence across different frequencies and directly maps the input series to the output series at each frequency component in frequency domain. **By leveraging disentangled representations in both the time and frequency domains, the model achieves reduced complexity with linear parameter growth and log-linear computational scaling. Additionally, as shown in Fig. 1d, these representations enhance domain experts’ trust by providing clear insights into the learned features and the**

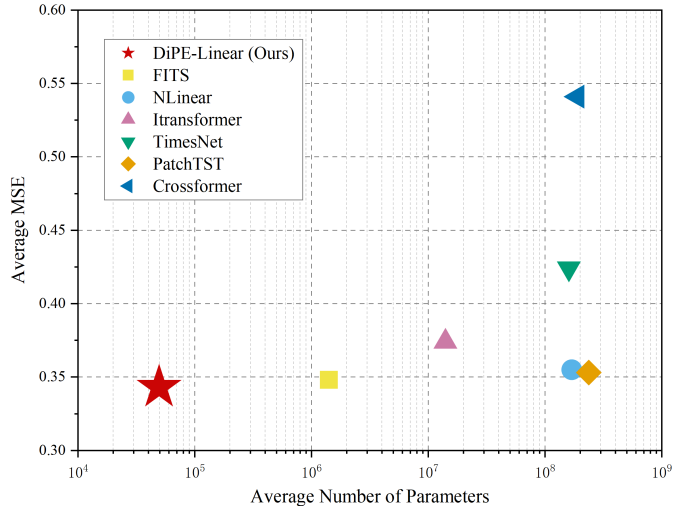


Fig. 2: Mean Squared Error (MSE) and number of parameters compared with other models. All results are taken as the average of 6 public LTSF datasets in horizon $L' = 720$ setting.

model’s reasoning process.

These sub-modules employ a **low-rank weight-sharing** policy to efficiently model inter-variate relationships, reducing model complexity while maintaining strong performance. We further introduce a novel loss function, **SFALoss**, which is defined as a sum of time-domain loss and frequency-domain loss weighted by frequency-domain attention in the SFA module, guiding the model to prioritize significant frequencies with less noise.

Additionally, by avoiding non-linearity within these modules, our model remains a linear model while achieving comparable or SOTA performance in LSTF with significantly fewer parameters, as shown in Fig. 2. This lightweight design enhances model’s interpretability and establishes a more reliable and efficient prediction pipeline, offering valuable insights for future research.

In summary, our contributions are multifold:

- We propose DiPE-Linear, a deep linear model that achieves efficiency, significantly reducing parameter complexity from quadratic to linear and computational complexity from quadratic to log-linear.
- Disentangled representation of model components in both time and frequency domain offers superior interpretability, thereby enhancing its trustworthiness for industrial applications.
- Extensive experiments demonstrate that our method outperforms existing approaches, offering superior performance, efficiency, and interpretability.

II. RELATED WORK

A. Efficient Architectures for Long-Term Forecasting

Long-term time series forecasting (LTSF) requires models capable of efficiently handling long sequences. Early

Transformer-based models [12]–[17] progressively reduced computational complexity from $\mathcal{O}(L^2)$ to $\mathcal{O}(L)$. However, due to the inherently complex structure of Transformers, these models still contain a large number of parameters and are highly prone to overfitting when dealing with excessively long input sequences in LTSF tasks [27].

DLinear [27] was the first to propose using a simple single-layer fully connected network to replace the complex Transformer structure. Although the fully connected layer has a computational complexity of $\mathcal{O}(L^2)$, its simple structure results in significantly lower complexity compared to other Transformer-based models. Nevertheless, DLinear still suffers from notable parameter redundancy. FITS [29] addressed this by employing low-pass filters to discard high-frequency information in the frequency domain, drastically reducing the number of parameters in the fully connected network to the scale of 10k. SparseTSF [37], on the other hand, introduced Cross-Period Sparse Forecasting, which achieves a parameter count on the scale of 1k through downsampling and cross-period parameter sharing. However, both FITS and SparseTSF sacrifice accuracy to achieve parameter reduction [37], [38]. Further exploration into addressing parameter redundancy in fully connected models remains an open research question.

B. Exploiting Frequency-Domain Characteristics

Recent advancements in time series forecasting have increasingly leveraged frequency-domain knowledge to improve performance. One prominent approach incorporates frequency-domain information as auxiliary features to enhance the modeling of long-term dependencies. For example, FEDformer [17] introduces a DFT-based frequency-enhanced attention mechanism, where attention weights are computed from the spectra of queries and keys, with the weighted sum calculated directly in the frequency domain. Similarly, FiLM [39] applies Fourier analysis to retain historical information while filtering out noise. Alternatively, some methods operate entirely in the frequency domain. FreTS [40] employs a frequency-domain MLP to capture both channel-wise and temporal dependencies, while FITS [29] adopts a fully connected network specifically designed for spectral representations.

Another promising direction incorporates frequency-domain loss functions into time-domain training objectives to capture spectral patterns more effectively. For example, FTMixer [26] and FreDF [41] add frequency-domain loss components on top of time-domain losses, enhancing the model’s ability to align with the ground truth in the frequency domain.

C. Channel-Independence for Multivariate Time Series

DLinear [27] was the first to introduce the Channel-Independent strategy for multivariate time series forecasting (the terms “channel” and “variate” are used interchangeably throughout this paper for simplicity). Although this approach ignores causal relationships between variables, it achieves significant performance improvements. PatchTST [19] further validated this idea in Transformer-based models, demonstrat-

ing that independently processing variables while sharing the same model weights across variables can be highly effective.

However, RLinear [28] shows that for variables with distinct periodic characteristics, using independent weights for each variable can further enhance performance. Subsequent research has focused on finding an optimal balance between weight sharing and weight independence. For instance, MLinear [42] dynamically adjusts between Weight Sharing and Weight Independent strategies based on the temporal semantics of different sequences, while CSC [43] reassigns weight-variable mappings during the validation phase to achieve variable clustering. Nevertheless, these methods come with limitations. MLinear requires calculating both Weight Sharing and Weight Independent outputs before combining them, which increases computational overhead. CSC, on the other hand, relies on a strong prior assumption that variables clustered together should share the same weights, which may not hold universally.

III. METHOD

DiPE-Linear is constructed from several essential components. We begin by outlining the preliminaries related to TSF and the Fourier Transform, providing the foundation for our approach. Next, we present the architecture of DiPE-Linear, detailing its three core modules: Static Frequential Attention (SFA), Static Temporal Attention (STA), and Independent Frequential Mapping (IFM), under assumption that the input series is univariate. Then, we describe how the Low-rank Weight Sharing method generalizes those modules to multivariate time series. Lastly, we introduce SFALoss, a novel loss function that combines weighted losses in both the frequency and time domains, guiding the model to prioritize informative patterns while enhancing predictive performance.

A. Preliminaries

1) *Problem Definition*: The multivariate TSF problem can be formally defined as follows: Given a historical time series $\mathbf{x} \in \mathbb{R}^{C \times L}$, where C is the number of variates and L is the look-back length of input time series, the objective is to predict the future time series $\mathbf{y} \in \mathbb{R}^{C \times L'}$, where L' is the forecasting horizon.

2) *Discrete Fourier Transform*: Time series data can be viewed as discrete samples of a continuous signal over time. In many signal processing and time-series forecasting applications, the Discrete Fourier Transform (DFT) is a commonly used method to analyze the frequency components of such discrete signals. For a discrete-time sequence $x[n]$ of length N , the DFT transforms the time-domain signal into its frequency-domain representation. This transformation is particularly useful for identifying underlying periodic patterns or extracting frequency components that contribute to the signal.

The DFT of a time series $x[n]$ is defined as:

$$X[k] = \sum_{n=0}^{N-1} x[n] e^{-j \frac{2\pi}{N} kn}, \quad k \in \llbracket 0, N-1 \rrbracket. \quad (1)$$

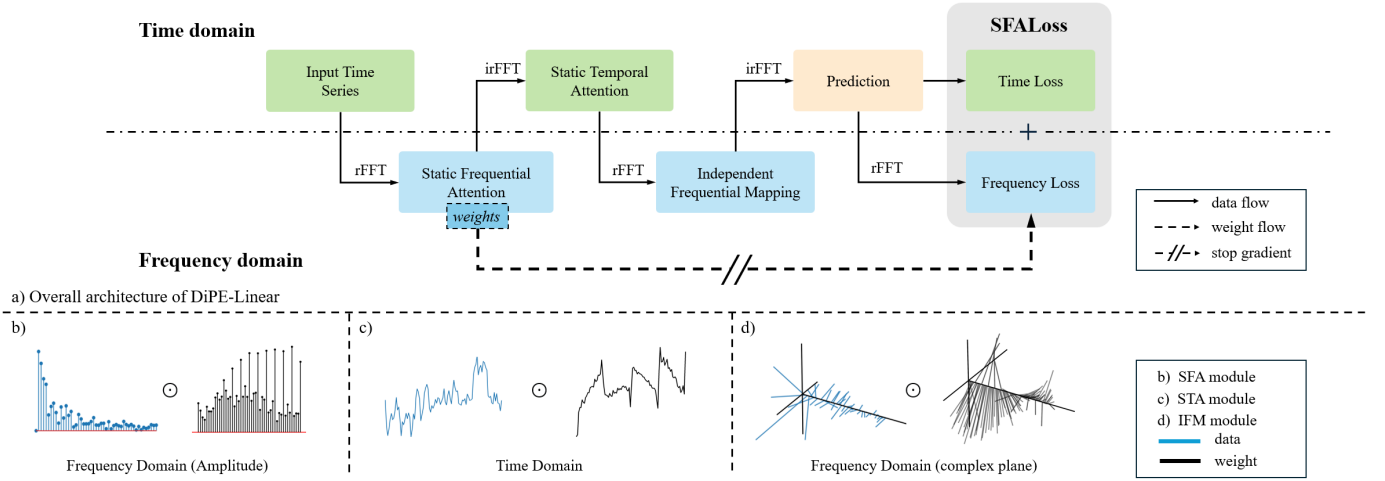


Fig. 3: Overall architecture of DiPE-Linear.

Once the signal is represented in the frequency domain, various operations, such as filtering or modifying specific frequency components, can be applied. The inverse Discrete Fourier Transform (iDFT) allows for transforming the modified frequency-domain signal back to the time domain. The iDFT is expressed as:

$$x[n] = \frac{1}{N} \sum_{k=0}^{N-1} X[k] e^{j \frac{2\pi}{N} kn}, \quad n \in \llbracket 0, N-1 \rrbracket. \quad (2)$$

This transformation provides the flexibility to manipulate signals in the frequency domain and revert them back to the time domain for further analysis or application. The ability to move between domains seamlessly is essential for efficient signal processing.

3) *Duality Between Time and Frequency Domains:* The DFT exhibits a fundamental property known as duality between the time and frequency domains. This duality manifests as convolution in the time domain being equivalent to multiplication in the frequency domain, and vice versa. For two time-domain signals, $x[n]$ and $h[n]$, their convolution:

$$y[n] = (x * h)[n] = \sum_{m=0}^{N-1} x[m] h[n-m] \quad (3)$$

has a frequency-domain equivalent:

$$Y[k] = X[k] \cdot H[k]. \quad (4)$$

Pointwise multiplication in the time domain, on the other hand, corresponds to convolution in the frequency domain. This relationship simplifies many operations, particularly in tasks where convolution is computationally intensive in the time domain.

Thus, the DFT provides a powerful tool for analyzing time series in the frequency domain, leveraging the duality between time and frequency domains to simplify complex operations

such as convolution. The ability to transition between domains efficiently enables advanced signal processing techniques for both single-channel and multichannel data.

B. Static Frequential Attention

Extracting frequencies is a common practice, as previous FITS [29] employed a low-pass filter to eliminate high-frequency signals, while FedFormer [17] randomly selects a subset of frequencies as key features. However, such strong prior assumptions may lead the model to discard useful information. Therefore, we aim for the model to learn which frequency components to focus on.

Specifically, to ensure the model's capability to select and amplify significant frequencies, we introduce SFA module as a frequency-domain filter. Additionally, to preserve the temporal structure of the series and avoid interference with subsequent temporal feature extraction, we constrained this filter to be a zero-phase filter. The SFA operates by first applying real Fast Fourier Transform (rFFT) to transform the time-domain data into the frequency domain. In this domain, a learned filter is applied via element-wise multiplication, selectively amplifying or suppressing specific frequency components. As a zero-phase filter, it exclusively modifies the amplitude of the signal while preserving the original phase information. Finally, inverse rFFT (irFFT) is used to reverse the filtered data back to the time domain. Specifically, the enhanced signal \mathbf{z}_{SFA} is given by

$$\mathbf{z}_{\text{SFA}} = \mathcal{F}^{-1}(\theta_{\text{SFA}} \odot \mathcal{F}(\mathbf{x})), \quad (5)$$

where $\mathbf{x} \in \mathbb{R}^L$ represents the input univariate series, \mathcal{F} denotes the rFFT, \mathcal{F}^{-1} is the irFFT, $\theta_{\text{SFA}} \in \mathbb{R}^{\lfloor L/2 \rfloor + 1}$ is the learnable static frequential attention map, and \odot denotes element-wise multiplication.

C. Static Temporal Attention

Similarly, to enable the model to have the capability of capturing important input time points in the temporal domain, we introduce the STA as a second component of our model. This module enables the input time series to undergo element-wise multiplication with a learned temporal attention map, effectively assigning appropriate importance to relevant historical time points and thereby enhancing the model's ability to capture temporal dependencies. The processed signal \mathbf{z}_{STA} is thus given by

$$\mathbf{z}_{\text{STA}} = \theta_{\text{STA}} \odot \mathbf{z}_{\text{SFA}}, \quad (6)$$

where $\theta_{\text{STA}} \in \mathbb{R}^L$ is the learnable time-domain attention map.

D. Independent Frequential Mapping

While both the SFA and STA modules function as part of the input series pre-processing, the IFM module directly maps the input historical series to the forecasted output. To process the time series as a whole, leveraging the spectrum is a natural approach, as it encapsulates all the information about the entire sequence and enables better handling of periodic components. Properly and efficiently processing the spectrum remains a key challenge. Fig. 1c illustrates that the two-dimensional matrix used by FITS [29] to handle the spectrum is sparse, with only the diagonal weights being significant. This suggests that, for a time series, there is relatively strong independence between different frequencies, allowing each frequency to be handled separately.

We thus treat each frequency independently for two key reasons: (1) Apart from harmonic frequencies, there is generally little correlation observed between different frequencies in time series data. [41] (2) Although harmonic frequencies tend to exhibit strong correlations, we avoid explicitly modeling these inter-frequency dependencies to mitigate potential multicollinearity in linear regression.

Therefore, for each frequency component, we apply a complex-valued multiply-accumulate operation independently. To transform the input space \mathbb{R}^L to the output space $\mathbb{R}^{L'}$, we apply zero-padding to the input series, extending its length to $L + L'$ before performing the rFFT. At the end, the last L' values are extracted and used as the predicted output. The forecasted output $\hat{\mathbf{y}}$ is thus defined as:

$$\mathbf{z}_{\text{STA_pad}} = \mathcal{F}(\text{zero_padding}(\mathbf{z}_{\text{STA}})) \quad (7)$$

$$\hat{\mathbf{Y}}_{\text{pad}} = \theta_{\text{IFM}} \odot \mathbf{z}_{\text{STA_pad}} + \beta_{\text{IFM}} \quad (8)$$

$$\hat{\mathbf{y}} = \mathcal{F}^{-1}(\hat{\mathbf{Y}}_{\text{pad}})_{[-L':]}, \quad (9)$$

where $\theta_{\text{IFM}} \in \mathbb{C}^{\lfloor (L+L'-1)/2 \rfloor + 1}$ is the complex-valued weight and $\beta_{\text{IFM}} \in \mathbb{C}^{\lfloor (L+L'-1)/2 \rfloor + 1}$ is the complex-valued bias.

This process can be equivalently described as a 1D convolution in time domain, as explained in equation 3 and 4:

$$\hat{\mathbf{y}} = \mathcal{F}^{-1}(\theta_{\text{IFM}}) * \mathbf{z}_{\text{STA}} + \mathcal{F}^{-1}(\beta_{\text{IFM}}), \quad (10)$$

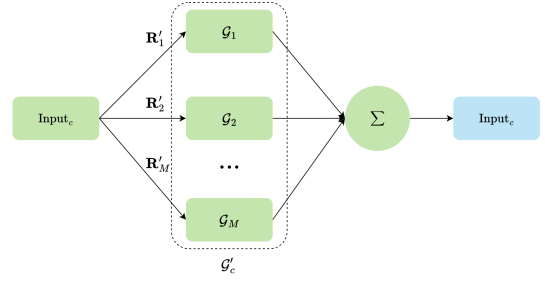


Fig. 4: Low-rank weight sharing architecture

where $\mathcal{F}^{-1}(\theta_{\text{IFM}}) \in \mathbb{R}^{L+L'-1}$ is the convolution kernel in time domain. The extremely large convolution kernel distinguishes it from traditional CNNs that use much smaller kernels. This larger kernel allows each output to capture a global receptive field, enabling the model to incorporate information from the entire input sequence.

E. Low-rank Weight Sharing

Weight sharing is a common practice in time series forecasting models [19], [27], [29], based on the assumption that different channels of a time series exhibit similar patterns. However, this assumption often does not hold. For example, in Weather datasets, variables such as temperature, pressure, and rainfall may follow distinct patterns. In such cases, training weights independently for each channel can improve performance [28], but this approach significantly increases the number of parameters by a factor of C , making the model complexity significantly higher.

To address this, we propose a more efficient alternative. By clustering variables based on their pattern similarities, we can reduce the number of weight sets, balancing the trade-off between model efficiency and performance. This clustering approach not only enhances computational efficiency by reducing the number of learned parameters but also improves accuracy, as the shared weights capture more robust patterns. Specifically, well-structured clustering ensures that the learned representations generalize better across similar variables. Inspired by mixture-of-experts [44] and dynamic convolution [45], we introduce a novel Low-rank Weight Sharing architecture, as shown in Fig. 4, leveraging these clustered patterns to optimize both parameter efficiency and predictive performance.

Specifically, for a multivariate time series with C variables, we introduce a hyperparameter M , where M denotes the number of independent weight sets to be learned, with $M \ll C$. For each component, M distinct sets of weights are learned, alongside a static routing matrix. The low-rank routing matrix $\mathbf{R} \in \mathbb{R}^{M \times C}$ is designed to linearly combine the weights and assign each variable to an appropriate weight set. We regularize the static routing matrix using the Softmax function, where τ is the Softmax temperature:

$$\mathbf{R}' = \text{Softmax}\left(\frac{\mathbf{R}}{\tau}\right). \quad (11)$$

We denote $\{\mathcal{G}_m\}_{m \in \llbracket 1, M \rrbracket}$ as the set of mappings representing any given module, corresponding to the M independent weight sets learned. For variate $c \in \llbracket 1, C \rrbracket$, the weight \mathcal{G}'_c actually applied to channel c is:

$$\mathcal{G}'_c = \sum_{m=1}^M \mathbf{R}'_c \cdot \mathcal{G}_m. \quad (12)$$

F. SFALoss

Building upon the insights of FreDF [41], we introduce SFALoss (denoted as \mathcal{L}), which combines Weighted Mean Absolute Error (WMAE) in the frequency domain (\mathcal{L}_F) and MSE in the time domain (\mathcal{L}_T). For the frequency domain component (\mathcal{L}_F), our SFA module selectively subtracts key frequencies while attenuating noisy frequencies. To refine this process, we modulate the frequency-domain loss \mathcal{L}_F through an element-wise multiplication with the SFA weighting factor, θ_{SFA} , effectively filtering out loss contributions from less relevant frequencies. The WMAE loss in the frequency domain \mathcal{L}_F is formulated as follows:

$$\mathcal{L}_F = \frac{1}{C} \sum_{c=1}^C \frac{\langle \mathbf{R}'_c \cdot \theta_{\text{STA}}, |\mathbf{Y}_c - \hat{\mathbf{Y}}_c| \rangle}{\|\mathbf{R}'_c \cdot \theta_{\text{STA}}\|_1}, \quad (13)$$

where $\mathbf{Y} = \mathcal{F}(\mathbf{y})$ and $\hat{\mathbf{Y}} = \mathcal{F}(\hat{\mathbf{y}})$ are respectively ground truth and predicted future time series in frequency-domain. While computing the loss, θ_{STA} is detached from the computational graph, ensuring that no gradients are backpropagated through it.

We also preserve the MSE loss in time domain \mathcal{L}_T :

$$\mathcal{L}_T = \frac{1}{C} \frac{1}{L'} \sum_{c=1}^C \sum_{i=1}^{L'} \|\hat{y}_{c,i} - y_{c,i}\|_2^2. \quad (14)$$

Finally, the overall SFALoss function is defined as follow:

$$\mathcal{L} = \alpha \mathcal{L}_F + (1 - \alpha) \mathcal{L}_T, \quad (15)$$

where $\alpha \in [0, 1]$ is hyperparameter that balances the contribution of the two loss terms, allowing us to achieve a trade-off between them.

IV. EXPERIMENT

A. Experimental Setup

1) *Dataset*: To comprehensively evaluate the performance and generalization capability of our model, we selected a diverse set of eight datasets, including six for LTSF and two for short-term time series forecasting (STSF). These datasets come from various domains, with different sizes and sampling frequencies, offering a robust benchmark for assessing the versatility and scalability of our approach across a wide range of forecasting tasks. Details are shown in Table I.

For the LTSF task, we utilized six public datasets:

TABLE I: Summary of LTSF and STSF datasets

Category	Dataset	Domain	Variates	Samples	Interval
LTSF	ETTh1	Industry	7	17420	1 hour
	ETTh2	Industry	7	17420	1 hour
	ETTh1	Industry	7	69680	15 min
	ETTh2	Industry	7	69680	15 min
	Electricity	Energy	321	26304	1 hour
	Weather	Environment	21	52696	1 hour
STSF	FaaS	Cloud Computing	1014	23041	1 min
	IaaS	Cloud Computing	168	69045	1 min
	Illness	Medical	7	966	1 week
	M5	Market	30	1941	1 day

- The **ETT**¹ dataset, including ETTh1, ETTh2, ETTm1 and ETTm2, comprises load and oil temperature data from two power transformers at different stations.
- The **Electricity**² dataset includes electricity consumption data, measured in kilowatt-hours (kWh), from 321 clients, spanning from 2012 to 2014.
- The **Weather**³ dataset consists of 21 meteorological indicators, sampled every 10 minutes, covering the entire year of 2020.

Moreover, to validate the effectiveness of the model in real-world production environments, we selected two workload dataset collected from ByteDance’s cloud servers, serving as private LTSF datasets:

- The **FaaS** includes 15-day query-per-second (QPS) data from the public cloud platform.
- The **IaaS** includes 45-day CPU usage data from the private cloud platform.

To further demonstrate the generalizability of our model, we extended our evaluation to two short-term forecasting tasks using the following datasets:

- The **Illness**⁴ dataset records weekly influenza-like illness cases as reported by the Centers for Disease Control and Prevention (CDC) in the United States, from 2002 to 2021.
- The **M5**⁵ dataset contains hierarchical sales data from Walmart, covering stores in three U.S. states.

2) *Implementation details*: All experiments are implemented in PyTorch [46] on an NVIDIA 4090D GPU. The models are trained using the Adam optimizer [47] with a learning rate of 0.001 for 50 epochs. Batch sizes are set to 64 and 8 for LTSF and STSF datasets, respectively. For Electricity and Weather datasets, $M = 4$, and $M = 1$ otherwise. Input sequence lengths L are 720, 2880, and 60 for public LTSF, private LTSF, and STSF datasets, respectively. Following [45], we apply linear annealing for the softmax temperature in Low-rank Weight Sharing to ensure balanced learning during early epochs.

¹<https://github.com/zhouhaoyi/ETDataset>

²<https://archive.ics.uci.edu/ml/datasets/ElectricityLoadDiagrams20112014>

³<https://www.bgc-jena.mpg.de/wetter/>

⁴<https://gis.cdc.gov/grasp/fluview/fluportaldashboard.html>

⁵<https://www.kaggle.com/competitions/m5-forecasting-accuracy/>

TABLE II: Forecasting results compared with FCs. A lower MSE or MAE is better. Average and standard deviation(\pm) of each metric are calculated over five runs. The best result is highlighted in **bold**, and the second best is highlighted with underline.

		DiPE-Linear (Ours)		FITS (ICLR-24)		RLinear (arXiv-23)		DLinear (AAAI-23)		NLinear (AAAI-23)	
Metrics		MSE	MAE	MSE	MAE	MSE	MAE	MSE	MAE	MSE	MAE
ETTh1	96	0.369 \pm 0.000	0.393 \pm 0.000	0.380 \pm 0.000	0.403 \pm 0.000	<u>0.376</u> \pm 0.004	<u>0.401</u> \pm 0.004	0.388 \pm 0.010	0.414 \pm 0.012	0.384 \pm 0.004	0.405 \pm 0.003
	192	0.407 \pm 0.000	0.415 \pm 0.000	0.417 \pm 0.001	0.425 \pm 0.001	0.416 \pm 0.002	0.426 \pm 0.002	0.425 \pm 0.005	0.436 \pm 0.005	0.415 \pm 0.003	0.424 \pm 0.002
	336	0.424 \pm 0.000	0.427 \pm 0.000	0.436 \pm 0.000	<u>0.440</u> \pm 0.000	0.444 \pm 0.002	0.444 \pm 0.002	0.469 \pm 0.010	0.469 \pm 0.009	0.445 \pm 0.002	0.443 \pm 0.002
	720	0.409 \pm 0.000	0.439 \pm 0.000	<u>0.432</u> \pm 0.000	<u>0.456</u> \pm 0.000	0.474 \pm 0.002	0.481 \pm 0.002	0.530 \pm 0.021	0.533 \pm 0.015	0.439 \pm 0.002	0.470 \pm 0.000
ETTh2	96	0.275 \pm 0.001	<u>0.336</u> \pm 0.001	<u>0.272</u> \pm 0.000	<u>0.336</u> \pm 0.000	0.270 \pm 0.001	0.335 \pm 0.001	0.280 \pm 0.005	0.345 \pm 0.004	0.276 \pm 0.002	0.338 \pm 0.001
	192	0.325 \pm 0.001	0.372 \pm 0.000	<u>0.331</u> \pm 0.000	<u>0.374</u> \pm 0.000	0.335 \pm 0.004	0.380 \pm 0.002	0.358 \pm 0.014	0.399 \pm 0.011	0.345 \pm 0.004	0.382 \pm 0.002
	336	0.350 \pm 0.002	0.393 \pm 0.001	<u>0.354</u> \pm 0.000	<u>0.395</u> \pm 0.000	0.366 \pm 0.005	0.409 \pm 0.003	0.439 \pm 0.017	0.457 \pm 0.009	0.375 \pm 0.009	0.411 \pm 0.004
	720	0.375 \pm 0.002	0.415 \pm 0.001	<u>0.378</u> \pm 0.000	<u>0.423</u> \pm 0.000	0.414 \pm 0.003	0.447 \pm 0.001	0.657 \pm 0.062	0.573 \pm 0.026	0.408 \pm 0.008	0.446 \pm 0.003
ETTh1	96	0.309 \pm 0.000	0.350 \pm 0.000	0.309 \pm 0.000	0.352 \pm 0.001	0.309 \pm 0.001	<u>0.352</u> \pm 0.001	<u>0.312</u> \pm 0.005	0.358 \pm 0.006	0.318 \pm 0.007	0.357 \pm 0.005
	192	0.339 \pm 0.000	0.369 \pm 0.000	0.339 \pm 0.001	0.369 \pm 0.001	<u>0.341</u> \pm 0.004	<u>0.370</u> \pm 0.003	0.350 \pm 0.006	0.386 \pm 0.008	0.350 \pm 0.007	0.377 \pm 0.005
	336	0.364 \pm 0.001	0.386 \pm 0.000	<u>0.368</u> \pm 0.001	0.386 \pm 0.001	0.369 \pm 0.003	<u>0.387</u> \pm 0.003	0.379 \pm 0.005	0.403 \pm 0.006	0.378 \pm 0.005	0.393 \pm 0.004
	720	<u>0.416</u> \pm 0.000	<u>0.413</u> \pm 0.000	<u>0.416</u> \pm 0.000	<u>0.413</u> \pm 0.000	0.415 \pm 0.001	0.411 \pm 0.001	0.439 \pm 0.011	0.443 \pm 0.012	0.420 \pm 0.003	0.415 \pm 0.002
ETTh2	96	0.162 \pm 0.000	<u>0.252</u> \pm 0.000	0.162 \pm 0.000	0.253 \pm 0.000	0.162 \pm 0.000	0.251 \pm 0.000	<u>0.163</u> \pm 0.001	0.255 \pm 0.001	0.162 \pm 0.000	<u>0.252</u> \pm 0.001
	192	0.216 \pm 0.000	0.289 \pm 0.000	0.216 \pm 0.000	0.291 \pm 0.000	0.216 \pm 0.000	<u>0.290</u> \pm 0.000	<u>0.219</u> \pm 0.002	0.297 \pm 0.001	0.216 \pm 0.000	0.291 \pm 0.000
	336	0.268 \pm 0.000	0.324 \pm 0.000	0.268 \pm 0.000	<u>0.326</u> \pm 0.000	0.268 \pm 0.001	<u>0.326</u> \pm 0.000	<u>0.272</u> \pm 0.003	0.334 \pm 0.003	0.268 \pm 0.000	<u>0.326</u> \pm 0.000
	720	<u>0.353</u> \pm 0.000	<u>0.379</u> \pm 0.000	0.349 \pm 0.000	0.378 \pm 0.000	0.354 \pm 0.001	0.384 \pm 0.000	0.367 \pm 0.004	0.398 \pm 0.003	0.349 \pm 0.000	<u>0.379</u> \pm 0.000
Electricity	96	0.132 \pm 0.000	0.228 \pm 0.001	0.134 \pm 0.000	0.231 \pm 0.000	0.135 \pm 0.000	0.232 \pm 0.000	<u>0.133</u> \pm 0.000	<u>0.229</u> \pm 0.000	0.133 \pm 0.000	0.228 \pm 0.000
	192	0.148 \pm 0.000	0.245 \pm 0.000	<u>0.149</u> \pm 0.000	0.244 \pm 0.000	0.150 \pm 0.000	0.246 \pm 0.000	0.148 \pm 0.000	<u>0.243</u> \pm 0.000	0.148 \pm 0.000	0.242 \pm 0.000
	336	0.162 \pm 0.000	0.261 \pm 0.000	0.165 \pm 0.000	<u>0.260</u> \pm 0.000	0.166 \pm 0.000	0.262 \pm 0.000	0.162 \pm 0.000	0.261 \pm 0.000	<u>0.164</u> \pm 0.000	0.258 \pm 0.000
	720	<u>0.198</u> \pm 0.002	0.296 \pm 0.001	0.204 \pm 0.000	<u>0.293</u> \pm 0.000	0.206 \pm 0.000	0.294 \pm 0.000	0.196 \pm 0.000	<u>0.293</u> \pm 0.001	0.203 \pm 0.000	0.291 \pm 0.000
Weather	96	0.142 \pm 0.001	0.201 \pm 0.001	0.142 \pm 0.000	0.192 \pm 0.000	<u>0.143</u> \pm 0.000	<u>0.194</u> \pm 0.000	0.142 \pm 0.000	0.202 \pm 0.000	0.142 \pm 0.001	0.192 \pm 0.001
	192	0.187 \pm 0.003	0.253 \pm 0.002	0.185 \pm 0.000	0.234 \pm 0.000	0.186 \pm 0.000	<u>0.235</u> \pm 0.000	<u>0.184</u> \pm 0.001	0.249 \pm 0.002	0.183 \pm 0.000	0.234 \pm 0.000
	336	0.234 \pm 0.001	0.293 \pm 0.002	<u>0.235</u> \pm 0.000	<u>0.276</u> \pm 0.000	0.236 \pm 0.000	0.275 \pm 0.000	0.236 \pm 0.001	0.293 \pm 0.001	0.234 \pm 0.001	<u>0.276</u> \pm 0.000
	720	0.306 \pm 0.004	0.348 \pm 0.003	<u>0.307</u> \pm 0.000	<u>0.328</u> \pm 0.000	0.308 \pm 0.000	0.327 \pm 0.000	0.306 \pm 0.002	0.349 \pm 0.002	0.308 \pm 0.000	0.330 \pm 0.000
FaaS	96	0.280 \pm 0.000	0.251 \pm 0.000	0.309 \pm 0.000	0.266 \pm 0.000	0.306 \pm 0.000	<u>0.264</u> \pm 0.000	<u>0.303</u> \pm 0.000	<u>0.264</u> \pm 0.000	0.305 \pm 0.000	0.266 \pm 0.000
	192	0.314 \pm 0.000	0.279 \pm 0.000	0.342 \pm 0.000	0.293 \pm 0.000	0.344 \pm 0.000	<u>0.292</u> \pm 0.000	<u>0.339</u> \pm 0.000	0.294 \pm 0.000	0.340 \pm 0.000	<u>0.292</u> \pm 0.000
	336	0.351 \pm 0.000	0.309 \pm 0.000	0.368 \pm 0.000	0.316 \pm 0.000	0.375 \pm 0.000	0.319 \pm 0.000	0.367 \pm 0.000	0.323 \pm 0.000	<u>0.364</u> \pm 0.000	<u>0.314</u> \pm 0.000
	720	0.379 \pm 0.000	0.332 \pm 0.000	0.415 \pm 0.000	0.348 \pm 0.000	0.436 \pm 0.000	0.350 \pm 0.000	0.417 \pm 0.000	0.364 \pm 0.001	<u>0.410</u> \pm 0.000	<u>0.344</u> \pm 0.000
IaaS	96	0.789 \pm 0.000	0.667 \pm 0.000	0.799 \pm 0.000	0.702 \pm 0.000	0.797 \pm 0.000	0.688 \pm 0.000	<u>0.795</u> \pm 0.000	0.699 \pm 0.000	0.799 \pm 0.000	<u>0.682</u> \pm 0.000
	192	0.817 \pm 0.000	0.698 \pm 0.000	0.839 \pm 0.000	0.723 \pm 0.000	<u>0.831</u> \pm 0.000	<u>0.700</u> \pm 0.000	0.823 \pm 0.000	0.717 \pm 0.000	0.820 \pm 0.000	0.702 \pm 0.000
	336	1.180 \pm 0.015	0.839 \pm 0.010	0.998 \pm 0.007	0.855 \pm 0.005	1.255 \pm 0.012	0.822 \pm 0.007	0.842 \pm 0.000	0.731 \pm 0.000	0.898 \pm 0.000	<u>0.771</u> \pm 0.000
	720	0.869 \pm 0.000	0.736 \pm 0.000	0.899 \pm 0.000	0.839 \pm 0.000	0.938 \pm 0.000	0.828 \pm 0.000	<u>0.881</u> \pm 0.000	<u>0.741</u> \pm 0.000	0.924 \pm 0.000	0.785 \pm 0.000
Illness	24	<u>2.260</u> \pm 0.000	<u>0.951</u> \pm 0.000	2.289 \pm 0.000	0.975 \pm 0.000	2.258 \pm 0.000	0.930 \pm 0.000	2.467 \pm 0.000	1.079 \pm 0.000	2.288 \pm 0.000	0.962 \pm 0.000
	36	2.162 \pm 0.000	0.940 \pm 0.000	2.292 \pm 0.000	0.986 \pm 0.000	<u>2.213</u> \pm 0.000	<u>0.943</u> \pm 0.000	2.510 \pm 0.000	1.089 \pm 0.000	2.221 \pm 0.000	0.964 \pm 0.000
	48	<u>2.184</u> \pm 0.000	0.956 \pm 0.000	2.266 \pm 0.000	0.992 \pm 0.000	2.309 \pm 0.000	0.979 \pm 0.000	2.510 \pm 0.000	1.092 \pm 0.000	2.177 \pm 0.000	<u>0.970</u> \pm 0.000
	60	2.053 \pm 0.000	<u>0.957</u> \pm 0.000	2.221 \pm 0.000	0.996 \pm 0.000	<u>2.183</u> \pm 0.000	0.952 \pm 0.000	2.599 \pm 0.000	1.121 \pm 0.000	2.216 \pm 0.000	0.985 \pm 0.000
M5	24	0.490 \pm 0.000	0.497 \pm 0.000	0.499 \pm 0.000	<u>0.502</u> \pm 0.000	0.500 \pm 0.000	0.503 \pm 0.000	0.503 \pm 0.000	0.505 \pm 0.000	<u>0.498</u> \pm 0.000	<u>0.502</u> \pm 0.000
	36	0.515 \pm 0.000	0.511 \pm 0.000	0.523 \pm 0.000	<u>0.529</u> \pm 0.000	0.524 \pm 0.000	0.517 \pm 0.000	0.533 \pm 0.000	0.521 \pm 0.000	<u>0.522</u> \pm 0.000	<u>0.515</u> \pm 0.000
	48	0.542 \pm 0.000	0.525 \pm 0.000	0.550 \pm 0.000	0.530 \pm 0.000	0.552 \pm 0.000	0.531 \pm 0.000	0.563 \pm 0.000	0.537 \pm 0.000	<u>0.549</u> \pm 0.000	<u>0.529</u> \pm 0.000
	60	0.565 \pm 0.000	0.538 \pm 0.000	0.572 \pm 0.000	0.542 \pm 0.000	0.575 \pm 0.000	0.543 \pm 0.000	0.581 \pm 0.000	0.547 \pm 0.000	<u>0.570</u> \pm 0.000	<u>0.541</u> \pm 0.000
Best count		32	26	<u>7</u>	5	<u>7</u>	<u>7</u>	6	1	9	6

3) *Baselines*: In this work, we focus on evaluating and comparing linear models, benchmarking our approach against leading methods such as FITS [29], RLlinear [28], DLinear, and NLinear [27]. To further demonstrate the effectiveness of our model, we also compare it with nonlinear deep learning models, including iTransformer [20], PatchTST [48], TimesNet [11], Crossformer [18], MICN [10], and FEDformer [17], showing that our model achieves state-of-the-art or comparable performance across both linear and nonlinear baselines. Additionally, SparseTSF [37] and FITS [29] are selected as parameter-efficient baselines to highlight the efficiency of our model design.

4) *Evaluation Metrics*: We follow the established practices in prior works to evaluate forecasting performance using two primary metrics: Mean Squared Error (MSE) and Mean

Absolute Error (MAE).

B. Main Results

1) *Versus FCs*: We first compared our model DiPE-Linear with other leading FCs. To ensure a fair evaluation, all models were trained using the same trainer settings. Throughout the training process, we carefully monitored each model to ensure convergence under these consistent conditions. All models use the optimal model hyperparameters provided in the authors' original implementations. Table II presents the evaluation results for the linear models on the LTSF and STSF datasets.

Across all eight datasets, DiPE-Linear consistently delivers comparable or even superior performance. On datasets with smaller sample sizes (ETTh1, ETTh2, FaaS, IaaS, Illness, and M5), our model significantly outperforms its counterparts,

TABLE III: Forecasting results compared with non linear models. A lower MSE or MAE is better. Metrics are averaged over five runs. Look-back length L is searched to the best for a fairer comparison. The best result is highlighted in **bold**, and the second best is highlighted with underline. Models marked by † use results as reported in ModernTCN [9].

		DiPE-Linear (Ours)		iTransformer (ICLR-24)		PatchTST† (ICLR-23)		TimesNet† (ICLR-23)		Crossformer† (ICLR-23)		MICN† (ICLR-23)		FEDformer† (ICML-22)	
Metrics		MSE	MAE	MSE	MAE	MSE	MAE	MSE	MAE	MSE	MAE	MSE	MAE	MSE	MAE
ETTh1	96	0.369	0.393	0.386	0.405	<u>0.370</u>	<u>0.399</u>	0.384	0.402	0.386	0.429	0.396	0.427	0.376	0.415
	192	0.407	0.415	0.424	0.440	<u>0.413</u>	<u>0.421</u>	0.557	0.436	0.419	0.444	0.430	0.453	0.423	0.446
	336	<u>0.424</u>	0.427	0.449	0.460	0.422	<u>0.436</u>	0.491	0.469	0.440	0.461	0.433	0.458	0.444	0.462
	720	0.409	0.439	0.495	0.487	<u>0.447</u>	<u>0.466</u>	0.521	0.500	0.519	0.524	0.474	0.508	0.469	0.492
ETTh2	96	<u>0.275</u>	0.336	0.297	0.348	0.274	0.336	0.340	0.374	0.276	<u>0.338</u>	0.289	0.357	0.332	0.374
	192	0.325	0.372	0.371	0.403	<u>0.339</u>	<u>0.379</u>	0.402	0.414	0.345	0.382	0.409	0.438	0.407	0.446
	336	<u>0.350</u>	<u>0.393</u>	0.404	0.428	0.329	0.380	0.452	0.452	0.375	0.411	0.417	0.452	0.400	0.447
	720	0.375	0.415	0.424	0.444	<u>0.379</u>	<u>0.422</u>	0.462	0.468	0.408	0.446	0.426	0.473	0.412	0.469
ETTM1	96	0.309	<u>0.350</u>	<u>0.300</u>	0.353	0.290	0.342	0.338	0.375	0.316	0.373	0.314	0.360	0.326	0.390
	192	<u>0.339</u>	0.369	0.345	<u>0.382</u>	0.332	0.369	0.371	0.387	0.377	0.411	0.359	0.387	0.365	0.415
	336	0.367	0.386	0.374	0.398	<u>0.369</u>	<u>0.392</u>	0.410	0.411	0.431	0.442	0.398	0.413	0.392	0.425
	720	0.416	0.413	<u>0.429</u>	0.430	0.416	<u>0.420</u>	0.478	0.450	0.600	0.547	0.459	0.464	0.446	0.458
ETTM2	96	0.162	0.252	0.175	0.266	<u>0.165</u>	<u>0.255</u>	0.187	0.267	0.421	0.461	0.178	0.273	0.180	0.271
	192	0.216	0.289	0.242	0.312	<u>0.220</u>	<u>0.292</u>	0.249	0.309	0.503	0.519	0.245	0.316	0.252	0.318
	336	0.268	0.324	0.282	0.340	<u>0.274</u>	<u>0.329</u>	0.321	0.351	0.611	0.580	0.295	0.350	0.324	0.364
	720	0.353	0.379	0.378	0.398	<u>0.362</u>	<u>0.385</u>	0.497	0.403	0.996	0.750	0.389	0.406	0.410	0.420
ECL	96	<u>0.132</u>	<u>0.228</u>	<u>0.132</u>	0.229	0.129	0.222	0.168	0.272	0.187	0.283	0.159	0.267	0.186	0.302
	192	<u>0.148</u>	<u>0.245</u>	<u>0.151</u>	0.246	0.147	0.240	0.184	0.289	0.258	0.330	0.168	0.279	0.197	0.311
	336	0.162	<u>0.261</u>	0.167	0.264	<u>0.163</u>	0.259	0.198	0.300	0.323	0.369	0.196	0.308	0.213	0.328
	720	0.198	0.296	0.194	0.286	<u>0.197</u>	<u>0.290</u>	0.220	0.320	0.404	0.423	0.203	0.312	0.233	0.344
Weather	96	0.142	<u>0.201</u>	0.159	0.208	<u>0.149</u>	0.198	0.172	0.220	0.153	0.217	0.161	0.226	0.238	0.314
	192	0.187	0.253	0.200	<u>0.248</u>	<u>0.194</u>	0.241	0.219	0.261	0.197	0.269	0.220	0.283	0.275	0.329
	336	0.234	0.293	0.253	<u>0.289</u>	<u>0.245</u>	0.282	0.280	0.306	0.252	0.311	0.275	0.328	0.339	0.377
	720	0.306	0.348	0.321	<u>0.338</u>	0.314	0.334	0.365	0.359	0.318	0.363	<u>0.311</u>	0.356	0.389	0.409
Best count		16	14	1	1	<u>8</u>	<u>11</u>	0	0	0	0	0	0	0	0

demonstrating its ability to effectively capture temporal patterns with limited training data while avoiding overfitting. On larger datasets (ETTh1, ETTm2, Electricity, and Weather), DiPE-Linear achieves results comparable to other linear models.

One notable advantage of DiPE-Linear is its substantially reduced parameter count compared to FCs. By operating within a low-dimensional manifold in the FCs’ model space, DiPE-Linear achieves performance comparable to or better than FCs, suggesting that our carefully designed model space contains the optimal solution to TSF tasks. This highlights the robustness and effectiveness of our architecture in representing the essential solution space of FCs with minimal complexity.

2) *Versus nonlinear models*: Next, we compare DiPE-Linear with several nonlinear models, including Transformer-based models and CNN-based models. Table III presents the evaluation results for these nonlinear models on public LTSF datasets. For private LTSF datasets, excessively long input lengths result in high memory usage for nonlinear models, leading to unacceptably high deployment costs in production environments. For STSF datasets, the limited amount of training data makes the models highly prone to overfitting, making training challenging. Therefore, we do not report model performance on these two types of datasets. To ensure a

fair comparison, all nonlinear models were trained with input lengths $L \in \{96, 192, 336, 512, 672, 720\}$, and the best results were selected for evaluation.

Our model demonstrates a slight performance advantage over PatchTST, while requiring only 10^{-4} times the parameter count. Furthermore, our model significantly outperforms other nonlinear models, highlighting its competitive advantages in both efficiency and performance.

3) *Parameter complexity and efficiency*: Recent studies have focused on parameter-efficient models, and we selected SparseTSF and FITS as baselines. In the FITS model, which employs a low-pass filter, we set the cutoff frequencies to the maximum and minimum harmonics provided in its source code, denoting them as FITS-T and FITS-L, respectively. Experiments on ETTh1, ETTm1, Electricity, and Weather datasets (Fig. 5) show that our model achieves the lowest MSE overall, with a parameter count falling between FITS-T and SparseTSF. While FITS-T reduces parameters by blocking more high-frequency information, it sacrifices performance. In contrast, our model not only uses fewer parameters than FITS-T but also matches or outperforms FITS-L. This demonstrates that our model design effectively balances performance and parameter efficiency for time series forecasting.

Table IV summarizes the parameter counts of leading mod-

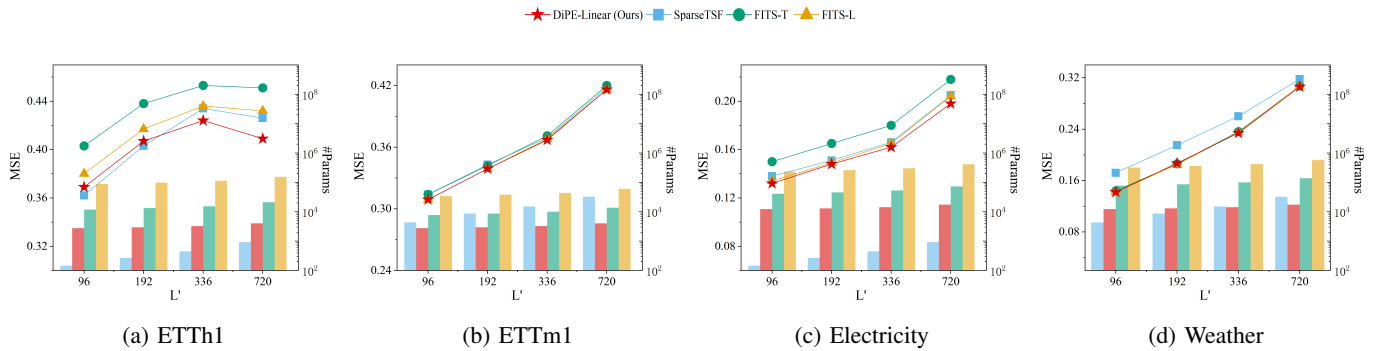


Fig. 5: Comparison of the number of parameters (bars) and MSE (lines) between parameter-efficient models.

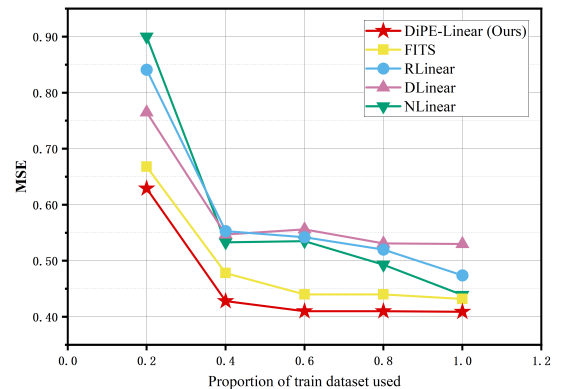
TABLE IV: Number of trainable parameters for look back length $L = 720$ and forecasting length $L' = 720$. Complex parameters are counted as double.

Model	ETTh1	ETTM1	Electricity	Weather
DiPE-Linear (Ours)	4K	4K	17K	16K
FITS	154K	60K	411K	572K
NLinear	519K	519K	519K	167M
RLinear	519K	519K	519K	167M
DLinear	1M	1M	1M	333M
iTransformer	1M	385K	5M	5M
TimesNet	1M	1M	151M	2M
PatchTST	36M	42M	40M	30M
Crossformer	43M	43M	18M	216K

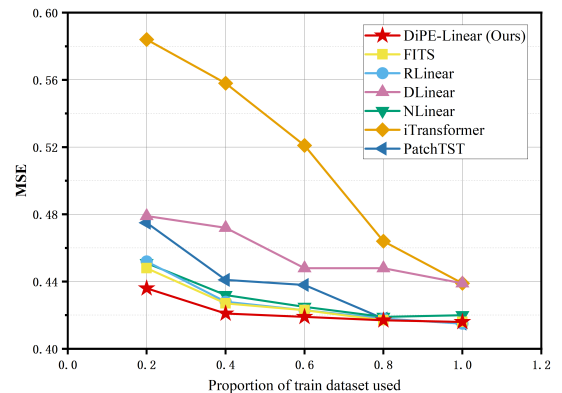
els on the LTSF dataset, using an input look-back length of $L = 720$ and an output length of $L' = 720$. DiPE-Linear emerges as the most lightweight model, with parameter counts reduced by a factor of 10^2 to 10^4 compared to other baseline models across four LTSF datasets. This compact design not only significantly lowers computational requirements but also aligns with environmentally sustainable practices by reducing the carbon footprint.

Fig. 2 further demonstrates the effectiveness of DiPE-Linear by comparing its average MSE and parameter counts with other baseline models across all prediction lengths and datasets. The results highlight that DiPE-Linear achieves state-of-the-art performance while maintaining a drastically smaller parameter count, underscoring its efficiency and practicality.

4) *Effect of Training Data Size*: To further investigate whether the model can perform effectively with reduced training data, we conducted experiments on the ETTh1 and ETTm1 datasets using different proportions of the training set. For the ETTh1 dataset, we compared our model with other FCs. Additionally, since the ETTm1 dataset contains more samples, we included nonlinear models for a broader comparison. As shown in Fig. 6, DiPE-Linear outperforms both FCs and nonlinear models across all proportions of the training set. Notably, on the ETTh1 dataset, our model surpasses the performance of other FC models trained on the full dataset while using only 40% of the training data.



(a) ETTh1



(b) ETTm1

Fig. 6: Impact of different proportion of train dataset used on ETT datasets.

C. Ablation Studies

1) *Basic Components*: To comprehensively validate the effectiveness of our model, we conducted ablation tests on two submodules: SFA and STA. The submodule IFM, which maps the input sequence space to the output sequence space, serves as the core component of our model and therefore cannot be ablated. Table V presents the results of the ablation experiments on the ETTh2 and Weather datasets with various

TABLE V: Ablation on components. MSE is used as the evaluation metric, and the best result in each row is highlighted in **bold**.

Components			ETTh2				Weather			
SFA	STA	IFM	96	192	336	720	96	192	336	720
\times	\checkmark	\checkmark	0.284	0.331	0.348	0.382	0.146	0.191	0.243	0.315
\checkmark	\times	\checkmark	0.290	0.331	0.348	0.379	0.166	0.220	0.272	0.331
\times	\times	\checkmark	0.295	0.340	0.352	0.387	0.175	0.228	0.274	0.332
\checkmark	\checkmark	\checkmark	0.275	0.325	0.350	0.375	0.142	0.187	0.234	0.306

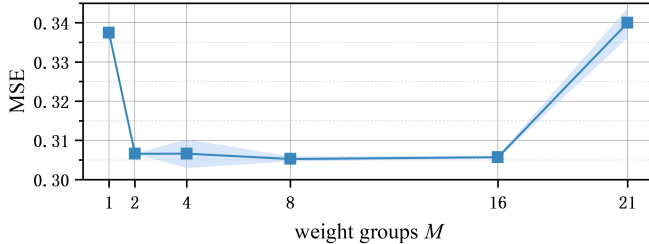


Fig. 7: Impact of varying rank M on MSE for prediction length $L' = 720$ on the weather dataset. Mean and standard deviation are calculated over five independent runs.

prediction lengths. In both the ETTh2 and Weather datasets, the incorporation of the SFA and STA modules generally enhances the model’s prediction accuracy. Specifically, in the Weather dataset, the abundance of training samples ensures that each submodule effectively captures significant patterns, leading to a substantial improvement in prediction performance. This demonstrates the necessity of addressing the importance of both the frequency domain and time domain in our input data processing.

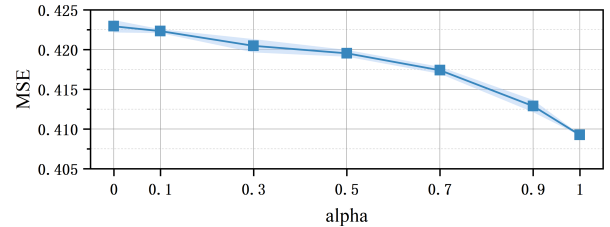
2) *Low-rank weight sharing*: In multivariate time series, our model must effectively capture the relationships between variables. We adopt a low-rank weight sharing approach, specifying the learning of M sets of weights. Figure 7 presents the results of testing different values of M on the Weather dataset with a prediction length of $L' = 720$. When $M = 1$, our model is equivalent to weight sharing, meaning all variables use the same set of weights. When $M = 21$, our model learns a separate set of weights for each variable, treating the variables as independent. The experiments indicate that selecting an appropriate value for M enables the model to achieve optimal performance.

We conducted an in-depth analysis to evaluate the necessity of low-rank weight sharing for each component of the model. Extensive experiments were performed on the ETTh2 and Weather datasets, covering multiple prediction horizons. For each component, we compared three configurations: shared weights, low-rank shared weights, and full-rank independent weights. As presented in Table VI, the low-rank weight sharing consistently delivered superior performance across all settings, highlighting its critical role in optimizing model efficacy.

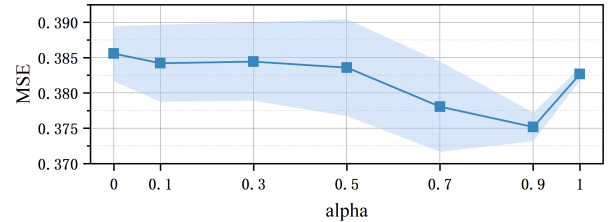
3) *SFALoss*: The parameter α in SFALoss governs the trade-off between the frequency domain loss and the time domain loss. To assess the influence of α on model perfor-

TABLE VI: Ablation on Low-rank weight sharing. \times denotes all variables share the same weights, \checkmark indicates low-rank weight sharing, and F represents full-rank independent weights for the component. MSE is used as the evaluation metric, and the best result in each row is highlighted in **bold**.

Components			ETTh2				Weather			
SFA	STA	IFM	96	192	336	720	96	192	336	720
\times	\checkmark	\checkmark	0.280	0.329	0.353	0.375	0.143	0.187	0.238	0.310
\checkmark	\times	\checkmark	0.279	0.326	0.354	0.374	0.142	0.187	0.238	0.309
\checkmark	\checkmark	\times	0.283	0.329	0.353	0.378	0.142	0.188	0.238	0.310
F	F	F	0.270	0.333	0.356	0.380	0.169	0.214	0.276	0.340
\checkmark	\checkmark	\checkmark	0.275	0.325	0.350	0.375	0.142	0.187	0.234	0.306



(a) ETTh1



(b) ETTh2

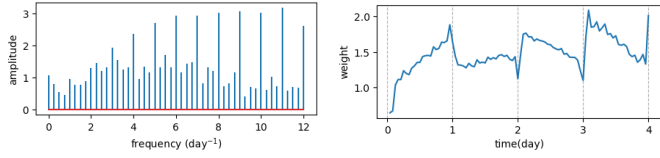
Fig. 8: MSE on different α setting on ETTh datasets. The forecast length $L' = 720$. Mean and standard deviation are calculated over five independent runs.

mance, we conducted experiments on the ETTh1 and ETTh2 datasets with a prediction length of $L' = 720$. The results, illustrated in Figure 8, demonstrate the significant impact of α on optimizing the model’s predictive accuracy across both datasets.

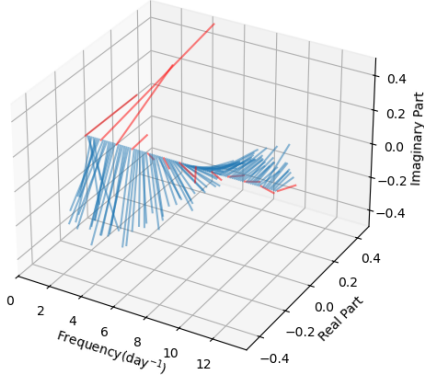
D. Interpretability: Case Studies

Benefiting from the disentangled representation of our model in both the frequency and time domains, our approach demonstrates superior interpretability. This interpretability facilitates user understanding of the model’s behavior, thereby enhancing trust in its predictive outcomes.

1) *ETTh1*: We select the ETTh1 dataset as a simple example. We choose an input length $L = 96$ and a prediction horizon $L' = 96$, ensuring the model has the minimum number of parameters. Additionally, within the ETTh1 dataset, we set the hyperparameter $M = 1$, which eliminates the router R . Thus for each module, we learn only a single set of weights. The weight visualization is shown in Fig. 9. The SFA module explicitly preserves low-frequency information while emphasizing harmonic amplitudes in the high-frequency region. The STA module identifies the importance of each



(a) SFA module in the frequency (b) STA module in the time domain.



(c) IFM module in the frequency domain - complex plane. Red lines represents the harmonics of the 1-day fundamental frequency.

Fig. 9: Weight visualization on the ETTh1 dataset with $M = 1$.

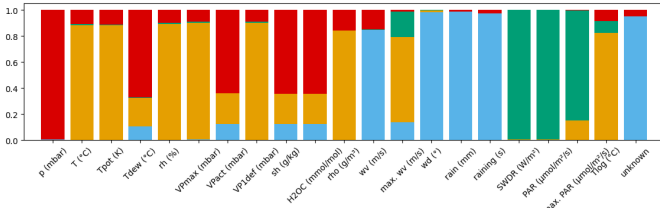


Fig. 10: Weight visualization of router R' on Weather dataset with $M = 4$.

time point in the input sequence for future predictions. The IFM module learns distinct prediction patterns for harmonic frequencies (shown in red) and non-harmonic frequencies (shown in blue).

2) *Weather*: In the Weather dataset, different variables represent various meteorological data, such as temperature, pressure, humidity, wind direction, precipitation, etc.. We set $M = 4$ as the hyperparameter, allowing the model to learn that the router can represent the correlations among different meteorological data variation patterns. The visualization is shown in Fig. 10.

We can further process the weights learned by the model to understand the knowledge it has captured. Taking the Router as an example, for each variable, the router weight R' can be viewed as the distribution of its predictive patterns across different weight groups. Consequently, we can compute the Jensen-Shannon Distance (JSD) between variables:

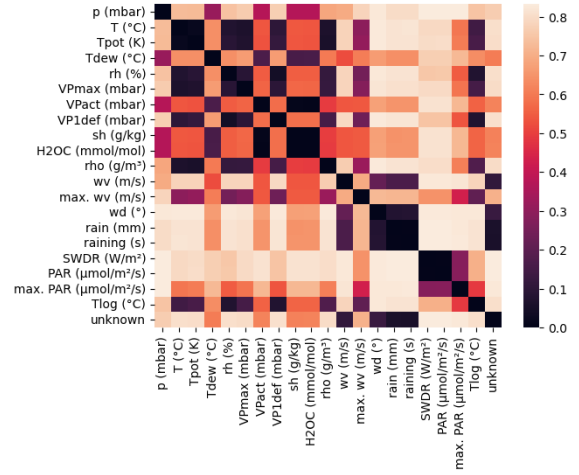


Fig. 11: Jensen-Shannon Distance matrix of router R' on the Weather dataset. Lower distance suggests similar forecasting mode.

$$\text{JSD}(R'_p \parallel R'_q) = \sqrt{\frac{1}{2}D_{\text{KL}}(R'_p \parallel O) + \frac{1}{2}D_{\text{KL}}(R'_q \parallel O)}, \quad (16)$$

where $p, q \in \{1, 2, \dots, C\}^2$ are two variables, $O = \frac{1}{2}(R'_p + R'_q)$ is a mixture distribution, and D_{KL} is the Kullback–Leibler (KL) divergence defined by (17):

$$D_{\text{KL}}(R'_p \parallel R'_q) = \sum_{i \in \{1, 2, \dots, M\}} R'_{p,i} \log \left(\frac{R'_{p,i}}{R'_{q,i}} \right). \quad (17)$$

Thus, we obtained the JSD Matrix based on the learnt router, as shown in Fig. 11.

3) *Electricity*: We further selected the Electricity dataset to comprehensively demonstrate the representations learned by DiPE-Linear. We chose an input length $L = 720$ and a prediction horizon $L' = 720$ in the LSTF setting. In the Electricity dataset, the hyperparameter $M = 4$, meaning that four sets of weights are learned for each module. The parameter visualization is shown in Figure 10. Similar to the ETTh1 dataset, the SFA module learns to retain low-frequency information and high-frequency harmonics. The STA module clearly distinguishes the periodic variations between weekdays and weekends within a month. In the IFM module, four different frequency transformation patterns are also learned. Finally, the weight visualization of the Router illustrates the differences and similarities in predictive patterns across different variables in the dataset.

E. Complexity analysis

Our model retains the linear characteristics of FCs while achieving significant reductions in both parameter and computational complexity. In this section, we analyze the complexity of each module in our model in detail. For simplicity, we denote ambiguously both the input length and forecast horizon as L .

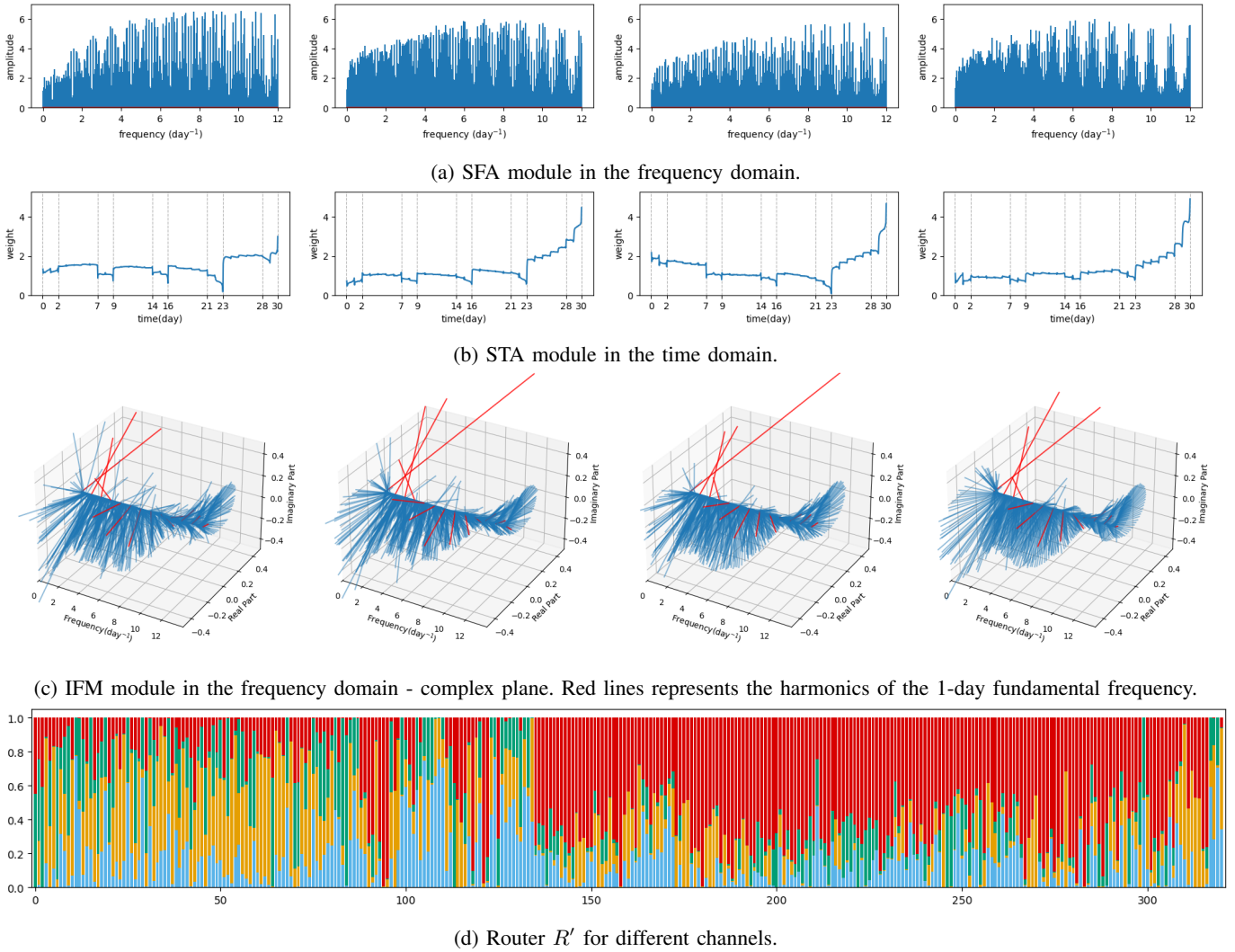


Fig. 12: Weight visualization on the Electricity dataset with $M = 4$.

1) *Parameter Complexity*: As shown in (5), (6) and (8), In the SFA, STA, and IFM modules, the parameter complexity is uniformly $\mathcal{O}(M \cdot L)$. Additionally, low-rank weight sharing introduces routing parameters with a complexity of $\mathcal{O}(M \cdot C)$, which is a higher-order infinitesimal relative to $\mathcal{O}(M \cdot L)$. Therefore, the overall model complexity is $\mathcal{O}(M \cdot L)$.

2) *Computational Complexity*: The computational cost of our model primarily arises from two components. First, the model's parameter computations involve only element-wise multiplications, yielding a computational complexity of $\mathcal{O}(C \cdot L)$. Second, the rFFT and iFFT operations each have a computational complexity of $\mathcal{O}(C \cdot L \log L)$. Therefore, the overall computational complexity of the model is $\mathcal{O}(C \cdot L \log L)$.

A comparison of the parameter and computational complexities between our model and FCs (both with and without weight sharing) is provided in Table VII.

TABLE VII: Comparison of parameter and time complexity with FCs. Note that $M \ll C \ll L$ in LTSF settings.

	DiPE-Linear (Ours)	FC (w/ sharing)	FC (w/o sharing)
Param.	$\mathcal{O}(M \cdot L)$	$\mathcal{O}(L^2)$	$\mathcal{O}(C \cdot L^2)$
Compu.	$\mathcal{O}(C \cdot L \log L)$	$\mathcal{O}(C \cdot L^2)$	$\mathcal{O}(C \cdot L^2)$

V. CONCLUSION

This paper presents DiPE-Linear, a novel approach designed for LTSF in industrial applications. DiPE-Linear effectively addresses the challenges of Industry 5.0, including high-dimensional and high-resolution data as well as high-stakes scenarios, by leveraging disentangled, linear-complexity interpretable modules in both the time and frequency domains. The sophisticated design reduces parameter complexity from quadratic to linear and computational complexity from quadratic to log-linear. Extensive experimental results demonstrate that DiPE-Linear consistently outperforms exist-

ing models, significantly enhancing scalability, computational efficiency, and predictive accuracy, particularly in complex industrial environments. In future work, we will enhance DiPE-Linear by incorporating interpretable nonlinear modules, while further exploring lightweight and efficient practical LSTF models.

REFERENCES

- [1] S. S. N. S. and S. V. D. K., "Time series forecasting of cloud resource usage," in *2021 IEEE 6th International Conference on Computing, Communication and Automation (ICCCA)*, 2021, pp. 372–382.
- [2] S. Ouhame, Y. Hadi, and A. Ullah, "An efficient forecasting approach for resource utilization in cloud data center using cnn-lstm model," *Neural Computing and Applications*, vol. 33, no. 16, pp. 10043–10055, 2021.
- [3] P. Lara-Benítez, M. Carranza-García, J. M. Luna-Romera, and J. C. Riquelme, "Temporal convolutional networks applied to energy-related time series forecasting," *applied sciences*, vol. 10, no. 7, p. 2322, 2020.
- [4] Y. Wang, R. Zou, F. Liu, L. Zhang, and Q. Liu, "A review of wind speed and wind power forecasting with deep neural networks," *Applied Energy*, vol. 304, p. 117766, 2021.
- [5] X. Zhou and X. Gao, "An attention-based forecasting network for intelligent services in manufacturing," in *Service-Oriented Computing: 19th International Conference, ICSSOC 2021, Virtual Event, November 22–25, 2021, Proceedings 19*. Springer, 2021, pp. 900–914.
- [6] A. Essien and C. Giannetti, "A deep learning model for smart manufacturing using convolutional lstm neural network autoencoders," *IEEE Transactions on Industrial Informatics*, vol. 16, no. 9, pp. 6069–6078, 2020.
- [7] S. Lin, W. Lin, W. Wu, F. Zhao, R. Mo, and H. Zhang, "Segrrn: Segment recurrent neural network for long-term time series forecasting," *arXiv preprint arXiv:2308.11200*, 2023.
- [8] M. Liu, A. Zeng, M. Chen, Z. Xu, Q. Lai, L. Ma, and Q. Xu, "Scinet: Time series modeling and forecasting with sample convolution and interaction," *Advances in Neural Information Processing Systems*, vol. 35, pp. 5816–5828, 2022.
- [9] L. donghao and wang xue, "ModernTCN: A modern pure convolution structure for general time series analysis," in *The Twelfth International Conference on Learning Representations*, 2024. [Online]. Available: <https://openreview.net/forum?id=vpJMJerXHU>
- [10] H. Wang, J. Peng, F. Huang, J. Wang, J. Chen, and Y. Xiao, "MICN: Multi-scale local and global context modeling for long-term series forecasting," in *The Eleventh International Conference on Learning Representations*, 2023. [Online]. Available: <https://openreview.net/forum?id=zt53IDUR1U>
- [11] H. Wu, T. Hu, Y. Liu, H. Zhou, J. Wang, and M. Long, "Timesnet: Temporal 2d-variation modeling for general time series analysis," in *The Eleventh International Conference on Learning Representations*, 2023. [Online]. Available: <https://openreview.net/forum?id=ju-Uqw384Oq>
- [12] S. Li, X. Jin, Y. Xuan, X. Zhou, W. Chen, Y.-X. Wang, and X. Yan, "Enhancing the locality and breaking the memory bottleneck of transformer on time series forecasting," in *Advances in Neural Information Processing Systems*, H. Wallach, H. Larochelle, A. Beygelzimer, F. d'Alché-Buc, E. Fox, and R. Garnett, Eds., vol. 32. Curran Associates, Inc., 2019. [Online]. Available: https://proceedings.neurips.cc/paper_files/paper/2019/file/6775a0635c302542da2c32aa19d86be0-Paper.pdf
- [13] N. Kitaev, L. Kaiser, and A. Levskaya, "Reformer: The efficient transformer," in *International Conference on Learning Representations*, 2020. [Online]. Available: <https://openreview.net/forum?id=rkgNKkHtvB>
- [14] H. Zhou, S. Zhang, J. Peng, S. Zhang, J. Li, H. Xiong, and W. Zhang, "Informer: Beyond efficient transformer for long sequence time-series forecasting," in *Proceedings of the AAAI conference on artificial intelligence*, vol. 35, no. 12, 2021, pp. 11 106–11 115.
- [15] H. Wu, J. Xu, J. Wang, and M. Long, "Autoformer: Decomposition transformers with auto-correlation for long-term series forecasting," *Advances in neural information processing systems*, vol. 34, pp. 22 419–22 430, 2021.
- [16] S. Liu, H. Yu, C. Liao, J. Li, W. Lin, A. X. Liu, and S. Dustdar, "Pyraformer: Low-complexity pyramidal attention for long-range time series modeling and forecasting," in *International Conference on Learning Representations*, 2022. [Online]. Available: <https://openreview.net/forum?id=0EXmFzUn5I>
- [17] T. Zhou, Z. Ma, Q. Wen, X. Wang, L. Sun, and R. Jin, "FEDformer: Frequency enhanced decomposed transformer for long-term series forecasting," in *Proceedings of the 39th International Conference on Machine Learning*, ser. *Proceedings of Machine Learning Research*, K. Chaudhuri, S. Jegelka, L. Song, C. Szepesvari, G. Niu, and S. Sabato, Eds., vol. 162. PMLR, 17–23 Jul 2022, pp. 27 268–27 286. [Online]. Available: <https://proceedings.mlr.press/v162/zhou22g.html>
- [18] Y. Zhang and J. Yan, "Crossformer: Transformer utilizing cross-dimension dependency for multivariate time series forecasting," in *The Eleventh International Conference on Learning Representations*, 2023. [Online]. Available: <https://openreview.net/forum?id=vSVLM2j9eie>
- [19] Y. Nie, N. H. Nguyen, P. Sinthong, and J. Kalagnanam, "A time series is worth 64 words: Long-term forecasting with transformers," in *The Eleventh International Conference on Learning Representations*, 2023. [Online]. Available: <https://openreview.net/forum?id=Jbc0vTocol>
- [20] Y. Liu, T. Hu, H. Zhang, H. Wu, S. Wang, L. Ma, and M. Long, "itransformer: Inverted transformers are effective for time series forecasting," in *The Twelfth International Conference on Learning Representations*, 2024. [Online]. Available: <https://openreview.net/forum?id=JePFAI8fah>
- [21] B. N. Oreshkin, D. Carпов, N. Chapados, and Y. Bengio, "N-beats: Neural basis expansion analysis for interpretable time series forecasting," 2020. [Online]. Available: <https://arxiv.org/abs/1905.10437>
- [22] C. Challu, K. G. Olivares, B. N. Oreshkin, F. Garza Ramirez, M. Mergenthaler Canseco, and A. Dubrawski, "Nhits: Neural hierarchical interpolation for time series forecasting," *Proceedings of the AAAI Conference on Artificial Intelligence*, vol. 37, no. 6, pp. 6989–6997, Jun. 2023. [Online]. Available: <https://ojs.aaai.org/index.php/AAAI/article/view/25854>
- [23] A. Das, W. Kong, A. Leach, S. K. Mathur, R. Sen, and R. Yu, "Long-term forecasting with tiDE: Time-series dense encoder," *Transactions on Machine Learning Research*, 2023. [Online]. Available: <https://openreview.net/forum?id=pCbC3aQB5W>
- [24] S.-A. Chen, C.-L. Li, S. O. Arik, N. C. Yoder, and T. Pfister, "TSMixer: An all-MLP architecture for time series forecasting," *Transactions on Machine Learning Research*, 2023. [Online]. Available: <https://openreview.net/forum?id=wbpxTuXgm0>
- [25] S. Wang, H. Wu, X. Shi, T. Hu, H. Luo, L. Ma, J. Y. Zhang, and J. Zhou, "Timemixer: Decomposable multiscale mixing for time series forecasting," 2024. [Online]. Available: <https://arxiv.org/abs/2405.14616>
- [26] Z. Li, Y. Qin, X. Cheng, and Y. Tan, "Ftmixer: Frequency and time domain representations fusion for time series modeling," 2024. [Online]. Available: <https://arxiv.org/abs/2405.15256>
- [27] A. Zeng, M. Chen, L. Zhang, and Q. Xu, "Are transformers effective for time series forecasting?" in *Proceedings of the AAAI conference on artificial intelligence*, vol. 37, no. 9, 2023, pp. 11 121–11 128.
- [28] Z. Li, S. Qi, Y. Li, and Z. Xu, "Revisiting long-term time series forecasting: An investigation on linear mapping," *arXiv preprint arXiv:2305.10721*, 2023.
- [29] Z. Xu, A. Zeng, and Q. Xu, "FITS: Modeling time series with \$10k\$ parameters," in *The Twelfth International Conference on Learning Representations*, 2024. [Online]. Available: <https://openreview.net/forum?id=bWcnvZ3qMb>
- [30] P. J. Lisboa, S. Saralajew, A. Vellido, R. Fernández-Domenech, and T. Villmann, "The coming of age of interpretable and explainable machine learning models," *Neurocomputing*, vol. 535, pp. 25–39, 2023.
- [31] D. Janardhanan and E. Barrett, "Cpu workload forecasting of machines in data centers using lstm recurrent neural networks and arima models," in *2017 12th International Conference for Internet Technology and Secured Transactions (ICITST)*, 2017, pp. 55–60.
- [32] A. Mozo, B. Ordozgoiti, and S. Gomez-Canaval, "Forecasting short-term data center network traffic load with convolutional neural networks," *PloS one*, vol. 13, no. 2, p. e0191939, 2018.
- [33] G. Makridakis, D. Kyriazis, and S. Plitsos, "Predictive maintenance leveraging machine learning for time-series forecasting in the maritime industry," in *2020 IEEE 23rd International Conference on Intelligent Transportation Systems (ITSC)*, 2020, pp. 1–8.
- [34] T. R. Gadekallu, P. K. R. Maddikunta, P. Boopathy, N. Deepa, R. Chenguoden, N. Victor, W. Wang, W. Wang, Y. Zhu, and K. Dev, "Xai for industry 5.0 -concepts, opportunities, challenges and future directions," *IEEE Open Journal of the Communications Society*, pp. 1–1, 2024.
- [35] I. Ahmed, G. Jeon, and F. Piccialli, "From artificial intelligence to explainable artificial intelligence in industry 4.0: A survey on what,

how, and where.” *IEEE Transactions on Industrial Informatics*, vol. 18, no. 8, pp. 5031–5042, 2022.

- [36] X. Zhang, S. Zhao, Z. Song, H. Guo, J. Zhang, C. Zheng, and W. Qiang, “Not all frequencies are created equal: Towards a dynamic fusion of frequencies in time-series forecasting,” in *Proceedings of the 32nd ACM International Conference on Multimedia*, 2024, pp. 4729–4737.
- [37] S. Lin, W. Lin, W. Wu, H. Chen, and J. Yang, “SparseTSF: Modeling long-term time series forecasting with $*1k*$ parameters,” in *Proceedings of the 41st International Conference on Machine Learning*, ser. *Proceedings of Machine Learning Research*, R. Salakhutdinov, Z. Kolter, K. Heller, A. Weller, N. Oliver, J. Scarlett, and F. Berkenkamp, Eds., vol. 235. PMLR, 21–27 Jul 2024, pp. 30211–30226. [Online]. Available: <https://proceedings.mlr.press/v235/lin24n.html>
- [38] W. Toner and L. N. Darlow, “An analysis of linear time series forecasting models,” in *Forty-first International Conference on Machine Learning*, 2024. [Online]. Available: <https://openreview.net/forum?id=x182CcbYaT>
- [39] T. Zhou, Z. Ma, xue wang, Q. Wen, L. Sun, T. Yao, W. Yin, and R. Jin, “FiLM: Frequency improved legendre memory model for long-term time series forecasting,” in *Advances in Neural Information Processing Systems*, A. H. Oh, A. Agarwal, D. Belgrave, and K. Cho, Eds., 2022. [Online]. Available: <https://openreview.net/forum?id=zTQdHSQUQWc>
- [40] K. Yi, Q. Zhang, W. Fan, S. Wang, P. Wang, H. He, N. An, D. Lian, L. Cao, and Z. Niu, “Frequency-domain MLPs are more effective learners in time series forecasting,” in *Thirty-seventh Conference on Neural Information Processing Systems*, 2023. [Online]. Available: <https://openreview.net/forum?id=iif9mGCTfy>
- [41] H. Wang, L. Pan, Z. Chen, D. Yang, S. Zhang, Y. Yang, X. Liu, H. Li, and D. Tao, “Fredf: Learning to forecast in frequency domain,” 2024. [Online]. Available: <https://arxiv.org/abs/2402.02399>
- [42] W. Li, X. Meng, C. Chen, and J. Chen, “Mlinear: Rethink the linear model for time-series forecasting,” 2023. [Online]. Available: <https://arxiv.org/abs/2305.04800>
- [43] Y. Peiwen and Z. Changsheng, “Is channel independent strategy optimal for time series forecasting?” 2023. [Online]. Available: <https://arxiv.org/abs/2310.17658>
- [44] R. Ni, Z. Lin, S. Wang, and G. Fanti, “Mixture-of-linear-experts for long-term time series forecasting,” in *Proceedings of the 27th International Conference on Artificial Intelligence and Statistics*, ser. *Proceedings of Machine Learning Research*, S. Dasgupta, S. Mandt, and Y. Li, Eds., vol. 238. PMLR, 02–04 May 2024, pp. 4672–4680. [Online]. Available: <https://proceedings.mlr.press/v238/ni24a.html>
- [45] Y. Chen, X. Dai, M. Liu, D. Chen, L. Yuan, and Z. Liu, “Dynamic convolution: Attention over convolution kernels,” in *Proceedings of the IEEE/CVF Conference on Computer Vision and Pattern Recognition (CVPR)*, June 2020.
- [46] A. Paszke, S. Gross, F. Massa, A. Lerer, J. Bradbury, G. Chanan, T. Killeen, Z. Lin, N. Gimelshein, L. Antiga et al., “Pytorch: An imperative style, high-performance deep learning library,” *Advances in neural information processing systems*, vol. 32, 2019.
- [47] D. P. Kingma, “Adam: A method for stochastic optimization,” *arXiv preprint arXiv:1412.6980*, 2014.
- [48] A. Dosovitskiy, L. Beyer, A. Kolesnikov, D. Weissenborn, X. Zhai, T. Unterthiner, M. Dehghani, M. Minderer, G. Heigold, S. Gelly, J. Uszkoreit, and N. Houlsby, “An image is worth 16x16 words: Transformers for image recognition at scale,” in *International Conference on Learning Representations*, 2021. [Online]. Available: <https://openreview.net/forum?id=YicbFdNTTy>
- [5] X. Zhou and X. Gao, “An attention-based forecasting network for intelligent services in manufacturing,” in *Service-Oriented Computing: 19th International Conference, ICSOC 2021, Virtual Event, November 22–25, 2021, Proceedings 19*. Springer, 2021, pp. 900–914.
- [6] A. Essien and C. Giannetti, “A deep learning model for smart manufacturing using convolutional lstm neural network autoencoders,” *IEEE Transactions on Industrial Informatics*, vol. 16, no. 9, pp. 6069–6078, 2020.
- [7] S. Lin, W. Lin, W. Wu, F. Zhao, R. Mo, and H. Zhang, “Segrnn: Segment recurrent neural network for long-term time series forecasting,” *arXiv preprint arXiv:2308.11200*, 2023.
- [8] M. Liu, A. Zeng, M. Chen, Z. Xu, Q. Lai, L. Ma, and Q. Xu, “Scinet: Time series modeling and forecasting with sample convolution and interaction,” *Advances in Neural Information Processing Systems*, vol. 35, pp. 5816–5828, 2022.
- [9] L. donghao and wang xue, “ModernTCN: A modern pure convolution structure for general time series analysis,” in *The Twelfth International Conference on Learning Representations*, 2024. [Online]. Available: <https://openreview.net/forum?id=vpJMJerXHU>
- [10] H. Wang, J. Peng, F. Huang, J. Wang, J. Chen, and Y. Xiao, “MICN: Multi-scale local and global context modeling for long-term series forecasting,” in *The Eleventh International Conference on Learning Representations*, 2023. [Online]. Available: <https://openreview.net/forum?id=zt53IDUR1U>
- [11] H. Wu, T. Hu, Y. Liu, H. Zhou, J. Wang, and M. Long, “Timesnet: Temporal 2d-variation modeling for general time series analysis,” in *The Eleventh International Conference on Learning Representations*, 2023. [Online]. Available: https://openreview.net/forum?id=ju_Uqw384Oq
- [12] S. Li, X. Jin, Y. Xuan, X. Zhou, W. Chen, Y.-X. Wang, and X. Yan, “Enhancing the locality and breaking the memory bottleneck of transformer on time series forecasting,” in *Advances in Neural Information Processing Systems*, H. Wallach, H. Larochelle, A. Beygelzimer, F. d’Alché-Buc, E. Fox, and R. Garnett, Eds., vol. 32. Curran Associates, Inc., 2019. [Online]. Available: https://proceedings.neurips.cc/paper_files/paper/2019/file/6775a0635c302542da2c32aa19d86be0-Paper.pdf
- [13] N. Kitaev, L. Kaiser, and A. Levskaya, “Reformer: The efficient transformer,” in *International Conference on Learning Representations*, 2020. [Online]. Available: <https://openreview.net/forum?id=rkgNKKHtVB>
- [14] H. Zhou, S. Zhang, J. Peng, S. Zhang, J. Li, H. Xiong, and W. Zhang, “Informer: Beyond efficient transformer for long sequence time-series forecasting,” in *Proceedings of the AAAI conference on artificial intelligence*, vol. 35, no. 12, 2021, pp. 11 106–11 115.
- [15] H. Wu, J. Xu, J. Wang, and M. Long, “Autoformer: Decomposition transformers with auto-correlation for long-term series forecasting,” *Advances in neural information processing systems*, vol. 34, pp. 22 419–22 430, 2021.
- [16] S. Liu, H. Yu, C. Liao, J. Li, W. Lin, A. X. Liu, and S. Dustdar, “Pyrformer: Low-complexity pyramidal attention for long-range time series modeling and forecasting,” in *International Conference on Learning Representations*, 2022. [Online]. Available: <https://openreview.net/forum?id=0EXmFzUn5I>
- [17] T. Zhou, Z. Ma, Q. Wen, X. Wang, L. Sun, and R. Jin, “FEDformer: Frequency enhanced decomposed transformer for long-term series forecasting,” in *Proceedings of the 39th International Conference on Machine Learning*, ser. *Proceedings of Machine Learning Research*, K. Chaudhuri, S. Jegelka, L. Song, C. Szepesvari, G. Niu, and S. Sabato, Eds., vol. 162. PMLR, 17–23 Jul 2022, pp. 27 268–27 286. [Online]. Available: <https://proceedings.mlr.press/v162/zhou22g.html>
- [18] Y. Zhang and J. Yan, “Crossformer: Transformer utilizing cross-dimension dependency for multivariate time series forecasting,” in *The Eleventh International Conference on Learning Representations*, 2023. [Online]. Available: <https://openreview.net/forum?id=vSVLM2j9ie>
- [19] Y. Nie, N. H. Nguyen, P. Sinthong, and J. Kalagnanam, “A time series is worth 64 words: Long-term forecasting with transformers,” in *The Eleventh International Conference on Learning Representations*, 2023. [Online]. Available: <https://openreview.net/forum?id=Jbdc0vTOcol>
- [20] Y. Liu, T. Hu, H. Zhang, H. Wu, S. Wang, L. Ma, and M. Long, “itransformer: Inverted transformers are effective for time series forecasting,” in *The Twelfth International Conference on Learning Representations*, 2024. [Online]. Available: <https://openreview.net/forum?id=JePFAI8fah>
- [21] B. N. Oreshkin, D. Carпов, N. Chapados, and Y. Bengio, “N-

REFERENCES

- beats: Neural basis expansion analysis for interpretable time series forecasting,” 2020. [Online]. Available: <https://arxiv.org/abs/1905.10437>
- [22] C. Challu, K. G. Olivares, B. N. Oreshkin, F. Garza Ramirez, M. Mergenthaler Canseco, and A. Dubrawski, “Nhits: Neural hierarchical interpolation for time series forecasting,” *Proceedings of the AAAI Conference on Artificial Intelligence*, vol. 37, no. 6, pp. 6989–6997, Jun. 2023. [Online]. Available: <https://ojs.aaai.org/index.php/AAAI/article/view/25854>
- [23] A. Das, W. Kong, A. Leach, S. K. Mathur, R. Sen, and R. Yu, “Long-term forecasting with tiDE: Time-series dense encoder,” *Transactions on Machine Learning Research*, 2023. [Online]. Available: <https://openreview.net/forum?id=pCbC3aQB5W>
- [24] S.-A. Chen, C.-L. Li, S. O. Arik, N. C. Yoder, and T. Pfister, “TSMixer: An all-MLP architecture for time series forecasting,” *Transactions on Machine Learning Research*, 2023. [Online]. Available: <https://openreview.net/forum?id=wbpxTuXgm0>
- [25] S. Wang, H. Wu, X. Shi, T. Hu, H. Luo, L. Ma, J. Y. Zhang, and J. Zhou, “Timemixer: Decomposable multiscale mixing for time series forecasting,” 2024. [Online]. Available: <https://arxiv.org/abs/2405.14616>
- [26] Z. Li, Y. Qin, X. Cheng, and Y. Tan, “Ftmixer: Frequency and time domain representations fusion for time series modeling,” 2024. [Online]. Available: <https://arxiv.org/abs/2405.15256>
- [27] A. Zeng, M. Chen, L. Zhang, and Q. Xu, “Are transformers effective for time series forecasting?” in *Proceedings of the AAAI conference on artificial intelligence*, vol. 37, no. 9, 2023, pp. 11 121–11 128.
- [28] Z. Li, S. Qi, Y. Li, and Z. Xu, “Revisiting long-term time series forecasting: An investigation on linear mapping,” *arXiv preprint arXiv:2305.10721*, 2023.
- [29] Z. Xu, A. Zeng, and Q. Xu, “FITS: Modeling time series with 10^6 parameters,” in *The Twelfth International Conference on Learning Representations*, 2024. [Online]. Available: <https://openreview.net/forum?id=bWcnvZ3qMb>
- [30] P. J. Lisboa, S. Saralajew, A. Vellido, R. Fernández-Domenech, and T. Villmann, “The coming of age of interpretable and explainable machine learning models,” *Neurocomputing*, vol. 535, pp. 25–39, 2023.
- [31] D. Janardhanan and E. Barrett, “Cpu workload forecasting of machines in data centers using lstm recurrent neural networks and arima models,” in *2017 12th International Conference for Internet Technology and Secured Transactions (ICITST)*, 2017, pp. 55–60.
- [32] A. Mozo, B. Ordozgoiti, and S. Gomez-Canaval, “Forecasting short-term data center network traffic load with convolutional neural networks,” *PloS one*, vol. 13, no. 2, p. e0191939, 2018.
- [33] G. Makridakis, D. Kyriazis, and S. Plitsos, “Predictive maintenance leveraging machine learning for time-series forecasting in the maritime industry,” in *2020 IEEE 23rd International Conference on Intelligent Transportation Systems (ITSC)*, 2020, pp. 1–8.
- [34] T. R. Gadekallu, P. K. R. Maddikunta, P. Boopathy, N. Deepa, R. Chenguoden, N. Victor, W. Wang, W. Wang, Y. Zhu, and K. Dev, “Xai for industry 5.0 -concepts, opportunities, challenges and future directions,” *IEEE Open Journal of the Communications Society*, pp. 1–1, 2024.
- [35] I. Ahmed, G. Jeon, and F. Piccialli, “From artificial intelligence to explainable artificial intelligence in industry 4.0: A survey on what, how, and where,” *IEEE Transactions on Industrial Informatics*, vol. 18, no. 8, pp. 5031–5042, 2022.
- [36] X. Zhang, S. Zhao, Z. Song, H. Guo, J. Zhang, C. Zheng, and W. Qiang, “Not all frequencies are created equal: Towards a dynamic fusion of frequencies in time-series forecasting,” in *Proceedings of the 32nd ACM International Conference on Multimedia*, 2024, pp. 4729–4737.
- [37] S. Lin, W. Lin, W. Wu, H. Chen, and J. Yang, “SparseTSF: Modeling long-term time series forecasting with 10^6 parameters,” in *Proceedings of the 41st International Conference on Machine Learning*, ser. *Proceedings of Machine Learning Research*, R. Salakhutdinov, Z. Kolter, K. Heller, A. Weller, N. Oliver, J. Scarlett, and F. Berkenkamp, Eds., vol. 235. PMLR, 21–27 Jul 2024, pp. 30 211–30 226. [Online]. Available: <https://proceedings.mlr.press/v235/lin24n.html>
- [38] W. Toner and L. N. Darlow, “An analysis of linear time series forecasting models,” in *Forty-first International Conference on Machine Learning*, 2024. [Online]. Available: <https://openreview.net/forum?id=x182CcbYaT>
- [39] T. Zhou, Z. Ma, xue wang, Q. Wen, L. Sun, T. Yao, W. Yin, and R. Jin, “FiLM: Frequency improved legendre memory model for long-term time series forecasting,” in *Advances in Neural Information Processing Systems*, A. H. Oh, A. Agarwal, D. Belgrave, and K. Cho, Eds., 2022. [Online]. Available: <https://openreview.net/forum?id=zTQdHSQUQWc>
- [40] K. Yi, Q. Zhang, W. Fan, S. Wang, P. Wang, H. He, N. An, D. Lian, L. Cao, and Z. Niu, “Frequency-domain MLPs are more effective learners in time series forecasting,” in *Thirty-seventh Conference on Neural Information Processing Systems*, 2023. [Online]. Available: <https://openreview.net/forum?id=iif9mGCTfy>
- [41] H. Wang, L. Pan, Z. Chen, D. Yang, S. Zhang, Y. Yang, X. Liu, H. Li, and D. Tao, “Fredf: Learning to forecast in frequency domain,” 2024. [Online]. Available: <https://arxiv.org/abs/2402.02399>
- [42] W. Li, X. Meng, C. Chen, and J. Chen, “Mlinear: Rethink the linear model for time-series forecasting,” 2023. [Online]. Available: <https://arxiv.org/abs/2305.04800>
- [43] Y. Peiwen and Z. Changsheng, “Is channel independent strategy optimal for time series forecasting?” 2023. [Online]. Available: <https://arxiv.org/abs/2310.17658>
- [44] R. Ni, Z. Lin, S. Wang, and G. Fanti, “Mixture-of-linear-experts for long-term time series forecasting,” in *Proceedings of The 27th International Conference on Artificial Intelligence and Statistics*, ser. *Proceedings of Machine Learning Research*, S. Dasgupta, S. Mandt, and Y. Li, Eds., vol. 238. PMLR, 02–04 May 2024, pp. 4672–4680. [Online]. Available: <https://proceedings.mlr.press/v238/ni24a.html>
- [45] Y. Chen, X. Dai, M. Liu, D. Chen, L. Yuan, and Z. Liu, “Dynamic convolution: Attention over convolution kernels,” in *Proceedings of the IEEE/CVF Conference on Computer Vision and Pattern Recognition (CVPR)*, June 2020.
- [46] A. Paszke, S. Gross, F. Massa, A. Lerer, J. Bradbury, G. Chanan, T. Killeen, Z. Lin, N. Gimelshein, L. Antiga et al., “Pytorch: An imperative style, high-performance deep learning library,” *Advances in neural information processing systems*, vol. 32, 2019.
- [47] D. P. Kingma, “Adam: A method for stochastic optimization,” *arXiv preprint arXiv:1412.6980*, 2014.
- [48] A. Dosovitskiy, L. Beyer, A. Kolesnikov, D. Weissenborn, X. Zhai, T. Unterthiner, M. Dehghani, M. Minderer, G. Heigold, S. Gelly, J. Uszkoreit, and N. Houlsby, “An image is worth 16x16 words: Transformers for image recognition at scale,” in *International Conference on Learning Representations*, 2021. [Online]. Available: <https://openreview.net/forum?id=YicbFdNTTy>